

## COMPOSITIONAL ANALYSIS OF SILICON

L.L. Kazmerski  
Solar Energy Research Institute  
Golden, Colorado 80401

## ABSTRACT

The use of surface analysis methods in the detection and evaluation of elemental and impurity species in Si is presented. Examples are provided from polycrystalline Si and high-efficiency MINP cells. Auger electron spectroscopy and secondary ion mass spectrometry are used to complement microelectrical data obtained by electron-beam induced-current measurements. A new method is discussed which utilizes the volume indexing of digital SIMS signals, providing compositional information and impurity maps on internal materials/device interfaces.

## I. INTRODUCTION

Impurities control the electro-optical properties of semiconductors and the operating lifetime and performance of solid-state devices. For such devices (including solar cells), it is important to know not only the levels of such impurities, but also their location and chemical state within the host lattice. A number of compositional characterization techniques are available to perform these analyses, mostly based on a bulk or volume scale. Surface analysis methods (1) - those that provide chemical and compositional information on the topmost atomic layers of a surface - have enhanced research and problem-solving in the semiconductor device area due to their complementary abilities to detect impurity (elemental, ionic, molecular) species, provide depth-compositional information (with ion-etching), determine chemical bonding states, map impurity localizations on surfaces or interfaces, and, evaluate integrity of interfaces. The common surface analysis techniques are summarized in Table 1. From this information, some of the strengths and limitations of the techniques can be deduced. For example, Auger electron spectroscopy (AES) can provide excellent spatial resolution due to the ability to focus the electron input probe. It lacks, however, the sensitivity to trace impurities which secondary ion mass spectrometry (SIMS) provides. X-ray photoelectron spectroscopy (XPS) complements these techniques in that it is the most developed and most reliable for providing chemical state information, with minimum inherent beam damage.

This paper focuses on the investigation of impurities in silicon solar cells, examining both single-crystal and polycrystalline types. The applications of AES and SIMS to elemental analysis in these devices are emphasized. Specifically, the interrelationships among the chemistry and composition of grains and grain boundaries, the electro-optical properties of the intergrain regions, and photovoltaic cell performance will be covered. The microelec-

00818-004

**Table 1. Summary of Selected Surface Analysis Techniques**

	<b>AES</b>	<b>EELS</b>	<b>SIMS</b>	<b>XPS</b>	<b>UPS</b>
<b>Probe</b>	electron	electron	Ion (+, -)	x-ray	ultraviolet
<b>Detected Species</b>	electron	electron	Ion (+, -)	electron	electron
<b>Spatial Resolution</b>	~300 Å	~300 Å	<1 µm	10 <sup>2</sup> - 10 <sup>3</sup> µm	~10 <sup>3</sup> µm
<b>Depth Resolution</b>	5 - 50 Å	5 - 50 Å	≥ 3 Å	5 - 50 Å	5 - 50 Å
<b>Detection Sensitivity</b>	0.1 at-%	0.1 at-%	<0.001 at-%	0.1 at-%	0.1 at-%

trical characterization of specific cell regions is accomplished by electron-beam-induced-current (EBIC) measurements, which provide information on the spatial distribution of current losses. Two impurity mechanisms are covered: (i) the segregation of oxygen (and other impurities) to the grain boundaries during heat treatments or high temperature processing of the devices. And, (ii) the passivation of the grain boundaries by incorporation of hydrogen in these regions. This hydrogen localization is determined directly and correlated with the microelectrical properties of these same regions, as well as cell performance. Of special interest is the introduction of a new method to detect and spatially-resolve impurities and elemental distributions within solid-state devices using digitally-acquired and indexed SIMS (2). This method permits the determination of impurity localization or distributions on internal device interfaces, with fracturing or otherwise exposing such areas. The utilization of this method in profiling higher efficiency Si cell's is exemplified.

## **II. OXYGEN SEGREGATION IN POLYCRYSTALLINE SILICON**

At the grain boundary, dislocations and bonding alterations make the material structurally and possibly chemically different than the bulk material in the grains. Thus the electrochemical potential in the grain boundary is generally different than in the grains. This potential difference provides a depletion region that can be the site of minority carrier recombination. The disruption can also provide a region for the localization of impurities, either from segregation of inherent species or of purposely-placed ones. The segregation of impurities to the intergrain regions has been demonstrated in cast and directionally-solidified Si (3). AES and SIMS has been utilized in conjunction with fracturing techniques to identify impurity species on the grain boundary planes. The fracturing process provides a method for the side-by-side analysis of a region - as indicated by the AES data of Fig. 1. However, inherent to this process is the loss of a large portion of the grain boundary plane. Because the electron probe can be scanned very effectively, impurity maps can be produced in the course of such AES (or SIMS) investigations. Such a mapping sequence is presented in Fig. 2. The benefit of this segregation process is that the grain regions themselves have significantly higher purity - with associated improvement of their electronic properties and device suitability. The grain boundary regions which act as sinks for such impurities are potential regions for enhanced minority carrier loss or impurity diffusion (shunting), but do not significantly degrade the cell performance unless impurity content is exceedingly high or the grain size is very small.

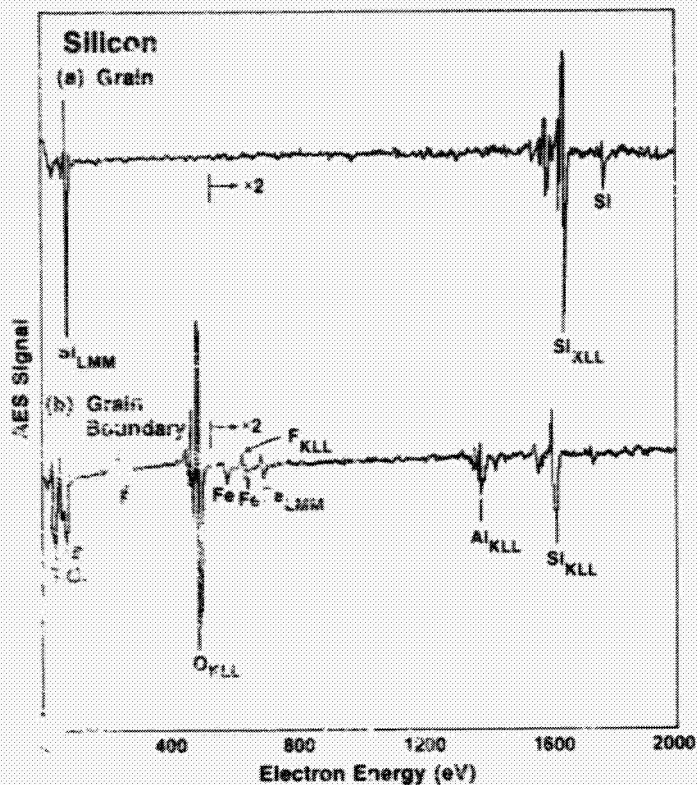
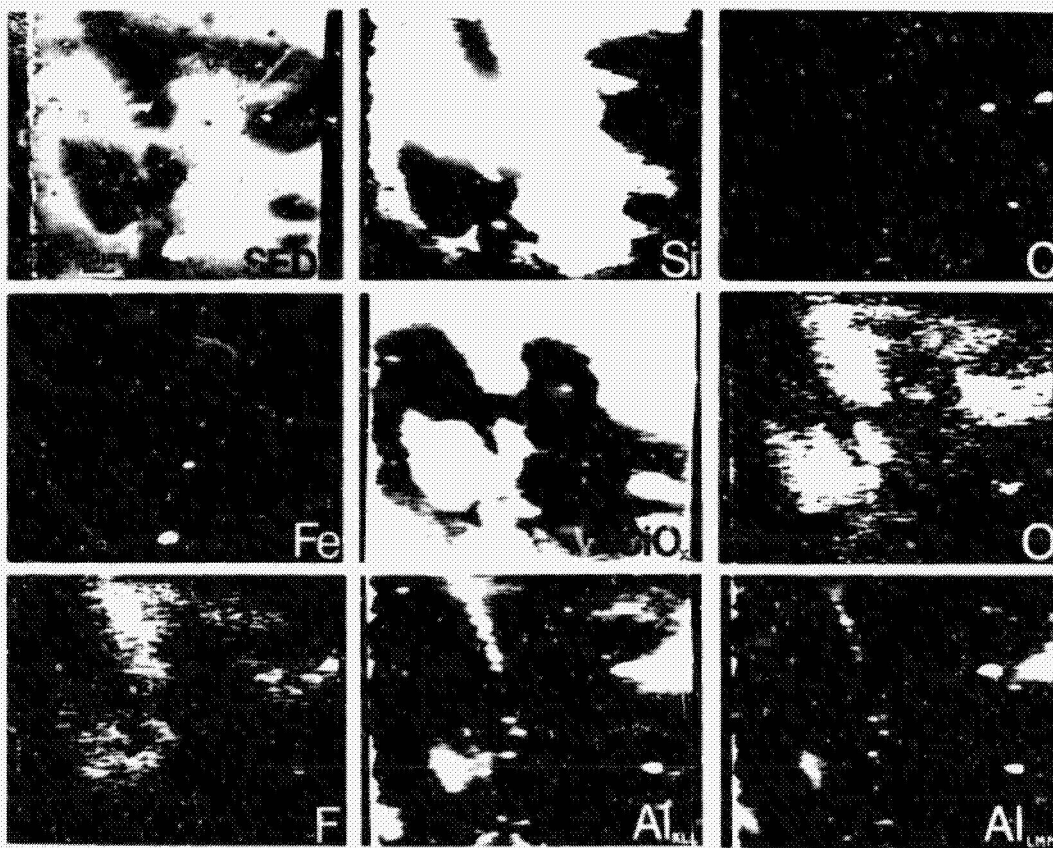


Fig. 1. AES surveys of fractured Si grain boundary: (a) grain region; (b) grain boundary.

ORIGINAL PAGE IS  
OF POOR QUALITY

Fig. 2. AES mapping sequence of impurities on fractured grain boundary.



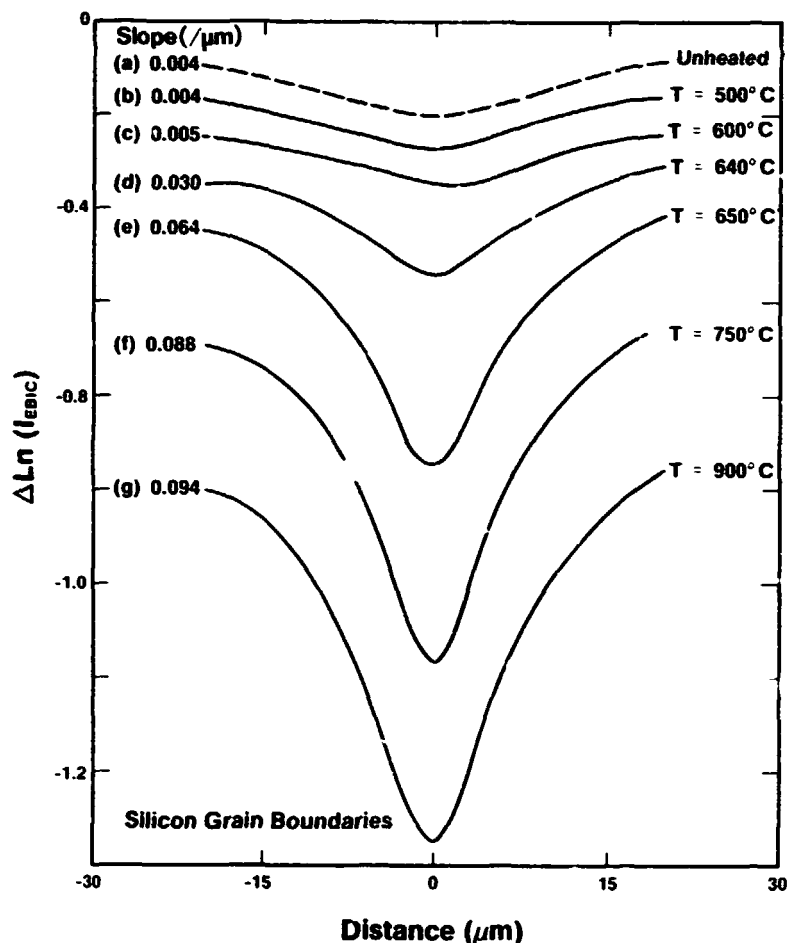
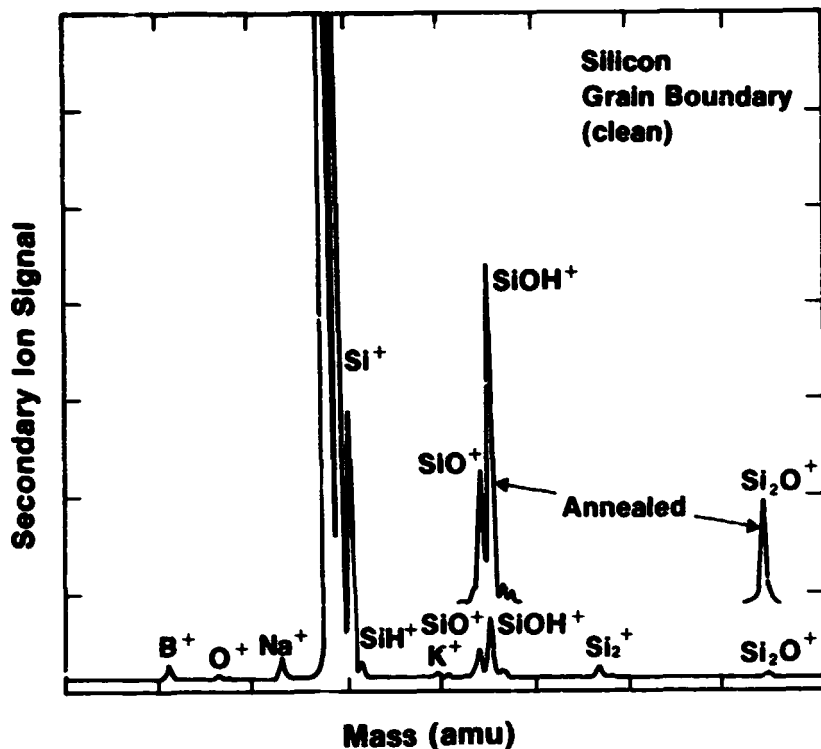


Fig. 3. EBIC linescans across Si grain boundaries as a function of thermal processing. Heat treatments are for 30 min in argon atmosphere.

The electrical activity of some grain boundaries in polycrystalline Si has been reported to be strongly affected by heat treatment (3,4). EBIC and compositional data from surface analysis measurements have been used to correlate the presences of oxygen at the grain boundaries with the electrical activation of these regions. The origin of the oxygen and resulting activity of the grain boundary is linked to the thermal history of the sample of devices (5). This is illustrated in the EBIC data of Fig. 3. The junction in this case is formed by an MIS structure fabricated on the individual grain boundary and adjacent grains at temperatures below 100°C in order to minimize additional thermal effects. The EBIC responses for unheated,  $T = 500^{\circ}\text{C}$ , and  $T = 600^{\circ}\text{C}$  cases are very similar, indicating that this mild thermal processing has little effect on the boundary region. If the temperature is increased, the EBIC responses increase correspondingly, indicating the electrical activation of these regions. The critical range for this activation is between  $600^{\circ}\text{C}$  and  $650^{\circ}\text{C}$ . Heating beyond  $900^{\circ}\text{C}$  does not seem to further affect the EBIC response, unless recrystallization occurs near the melting temperature. The slope of the  $\text{Ln}(I_{\text{EBIC}})$  vs. distance curves relates to the values of grain boundary recombination velocity ( $S_{\text{gb}}$ ) and effective diffusion length ( $L_{\text{eff}}$ ) (6). The existence of oxygen at the grain boundaries of annealed Si has been demonstrated using fracturing with SIMS. Figure 4 shows such data for an unannealed sample and one heated to  $750^{\circ}\text{C}$ . Increases in the oxide-signals (e.g., the  $\text{SiO}^{44}$  peak) are apparent. However, the fracturing process is difficult, and has less-than-desired repeatability and control.



Fig. 4. SIMS survey of unannealed and annealed grain boundaries.



### III. VOLUME INDEXING OF IMPURITIES AND ELEMENTS

The ability to reliably detect, map and quantify elemental or compositional information at regions within a solid-state device has been accomplished by the method illustrated in Fig. 5. In this, selected ion signals corresponding to elements or molecules of interest, are measured and stored (indexed for intensity, spatial location) digitally for an incremental volume encompassing the region or interface under analysis. A computer can be used to track the region of interest (e.g., grain boundary plane) by maximizing the presence of impurities which are known to exist in such regions. Thus, the internal interface can be exposed by spatially transforming the detected signals - even though the sputter profiling/SIMS operation is carried out at some angle to this plane. This avoids the loss of information experienced in the fracturing technique. The data can be coded for ion type, spatial origin ( $X$ ,  $Y$ ,  $Z$ ) and concentration level. Additionally, the results can be color coded for more effective presentation.

A simple example, which utilizes the depth profiling capabilities of the technique, is presented in Fig. 6. These data show the cross-sectional distribution of impurities in a high-efficiency Si MINP solar cell. The device structure has a double layer (ZnS/MgF) anti-reflection coating. A thin Si-oxide layer ( $\sim 30$  Å) covers the phosphorous-diffused, boron-doped substrate. The relevant secondary ion species utilized in the profiling sequence designated in Fig. 6. The expanded view of the oxide-semiconductor region illustrate the uniformity of the oxide itself. Because only a black/white

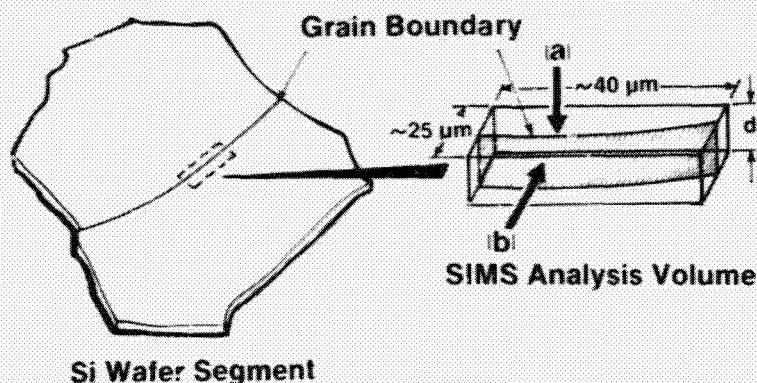


Fig. 5. Representation of SIMS volume indexing scheme.

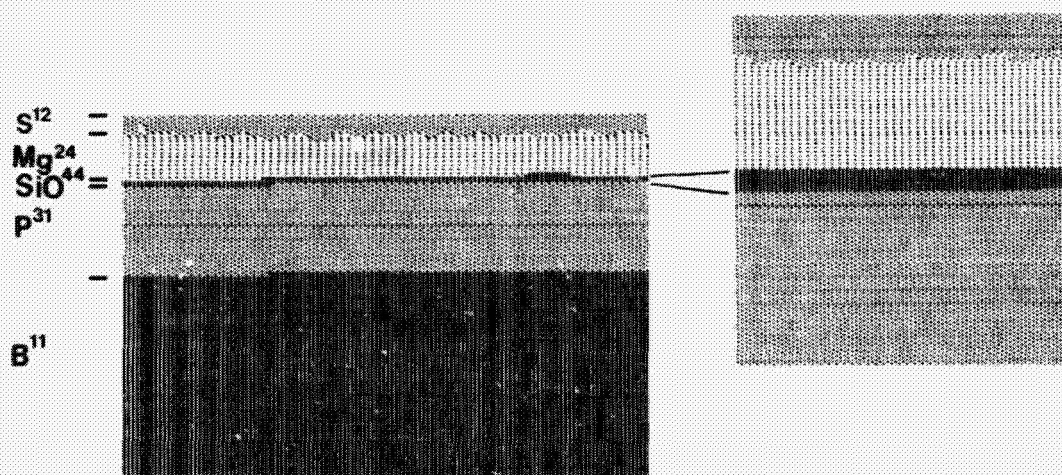


Fig. 6. Cross-section SIMS profile of Si MINP structure.

illustration is permitted in this publication, the relative concentrations are not indexed to ensure clarity. However, the phosphorous distribution is shown to peak at about  $10^{20}/\text{cm}^3$ , with a minimum of  $10^{17}/\text{cm}^3$  detected in Fig. 6. Same interdiffusion of the ARC is also observable.

This method has also been effective for investigation the segregation of oxygen in polycrystalline Si with heat treatment. The data presented in Fig. 7 are obtained by translating the volume-indexed SIMS data in order to view the boundary from "b" in Fig. 5. Again, the black and white format required for this paper has prevented the unambiguous coding for concentration level, and the data presented in Fig. 7 represent a threshold of  $1 \times 10^{17}/\text{cm}^2$  for  $\text{SiO}^{44}$  and  $1 \times 10^{18}/\text{cm}^3$  for C. Figure 7a represents the grain boundary plane for a boundary heated to  $600^\circ\text{C}$ . The solid black regions are carbon, and are decorated by oxygen--as indicated by the intense dot pattern from the  $\text{SiO}^{44}$  SIMS signal. The presence of any Si-O content for grain boundaries processed

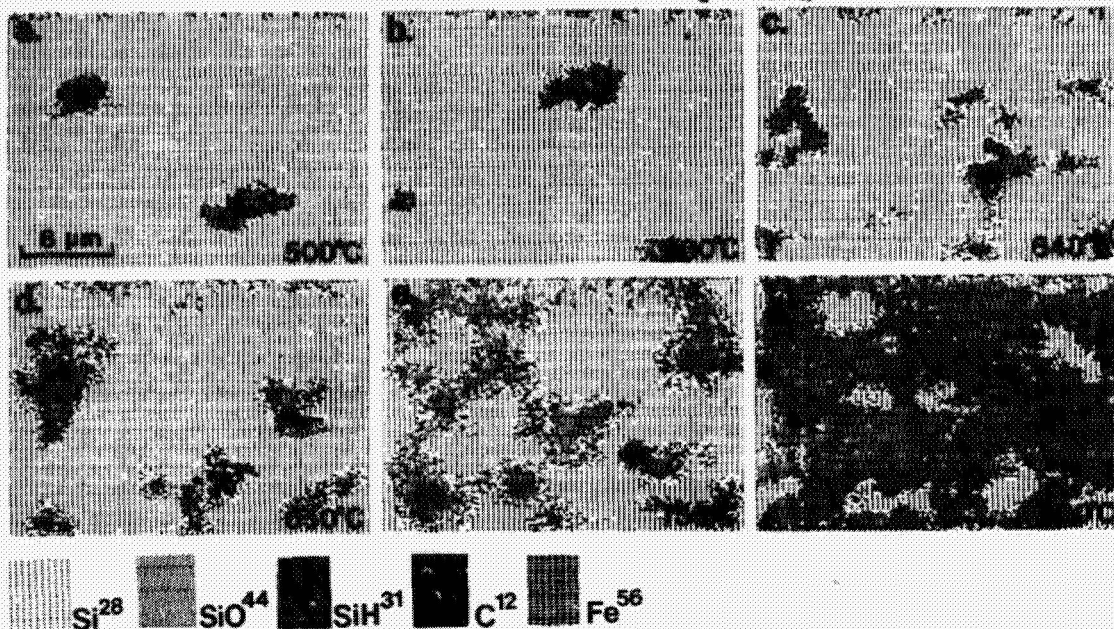


Fig. 7. SIMS mapping sequence of Si grain boundary showing oxygen segregation as a function of heat treatment. Impurity species key is included.

below 500°C is usually at some segregated impurity species (e.g., C, Fe, Ni, Al). As the annealing temperature is increased, the amount of oxygen at the boundary is observed to increase. Such data are shown in Figs. 7b-f, and correlate directly with the electrical activation of these regions determined by EBIC (Fig. 3). Spatially-resolved-minority carrier lifetime measurements, and the determination of the grain boundary barrier height have been reported (4,5) and directly complement these results. Thus, the segregation of oxygen to the grain boundaries results from high-temperature material/cell processing, and appears to be the origin of the electrical activation of these regions.

#### IV. HYDROGEN PASSIVATION

The effectiveness of hydrogen treatment on altering the electrical properties of polycrystalline Si and in improving the operational characteristics of cells has been demonstrated. The effect of such hydrogen processing is shown in the J-V characteristics of Fig. 8. The cell undergoes a change in efficiency from 5.8% to 7.7% (no antireflection coating) upon hydrogen treatment. Although the phenomenological effects of the hydrogen processing on cell improvement have been observed, little is known about the incorporation of this impurity species into the grain boundary or its possible interaction with the segregated oxygen that might be present in that region. Dube, et al. (7) have shown that hydrogen does alter the EBIC response of representative devices. They have deduced a diffusion coefficient for H in the Si grain boundary by examining the boundary from the side and along its length.



This analysis does not detect hydrogen directly, and assumes that the hydrogen is indeed localized there and responsible for the response. Figure 9 shows the effect of hydrogen treatment on a specific grain boundary. The EBIC response of Fig. 9a is for a decrease significantly with hydrogen treatment (Fig. 9b). Reheating this same boundary to 900°C "restores" the active response, but the magnitude is decreased somewhat. A second hydrogen treatment passivates the region again, with the response slightly less than after the initial hydrogen processing. These data are complemented by the grain boundary barrier height vs. light irradiation data of Fig. 10. The sequence is (a) unannealed grain boundary; (b) hydrogen-treated; (c) annealed, 900°C; (d) second hydrogen treatment; (e) annealed, 900°C; and, (f) third hydrogen treatment. The barrier height is improved, and becomes less sensitive to light intensity after the hydrogen passivation. In addition, the barrier height is observed to decrease with each successive hydrogen processing.

The incorporation of the hydrogen in the grain boundary and the relationship between the hydrogen and oxygen concentrations in that region are illustrated in Figs. 11-15. Figure 11 presents conventional SIMS depth-compositional profiles of hydrogen, measured by the magnitude of the  $\text{SiH}^{31}$  peak (with a threshold of  $10^{18}/\text{cm}^2$  in these figures). The  $\text{Si}^{28}$  peak is provided for reference. Figure 11a, b and c represent data on similar grain boundaries hydrogen-processed for 1, 2 and 4 minutes. Figure 12 provides similar data taken on a grain boundary (a) before and (b) after hydrogen passivation. A generally constant  $\text{SiO}^{44}$  signal is measured before the hydrogen processing. Since previous data have shown that the heat treatment and correlated oxygen segregation is primarily responsible for the activation of grain boundary electrical response, it is proposed that the hydrogen passivation is a result of the chemical interaction of the species at the grain boundary plane.

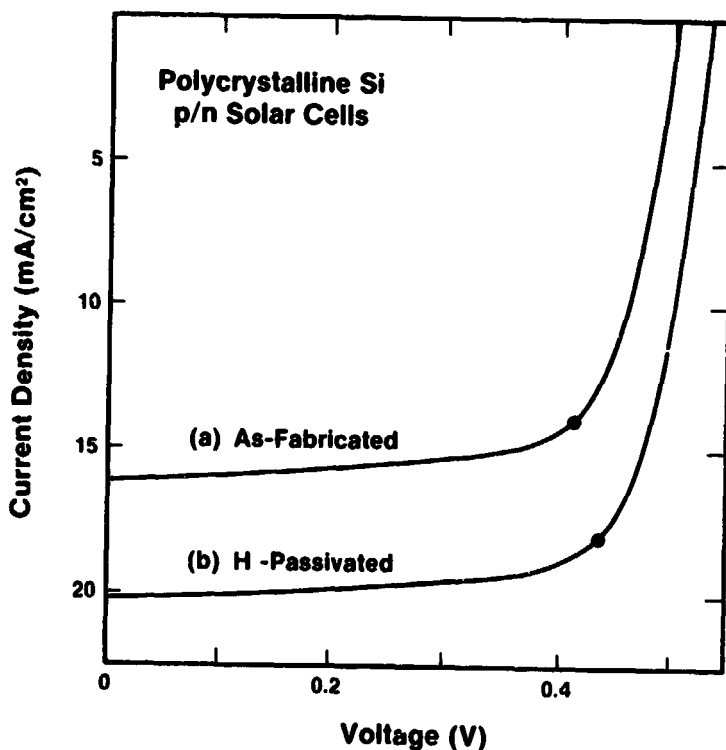


Fig. 8. Light current-voltage characterization for polycrystalline Si solar cells: (a) as fabricated; (b)  $\text{H}_2$ -passivated.

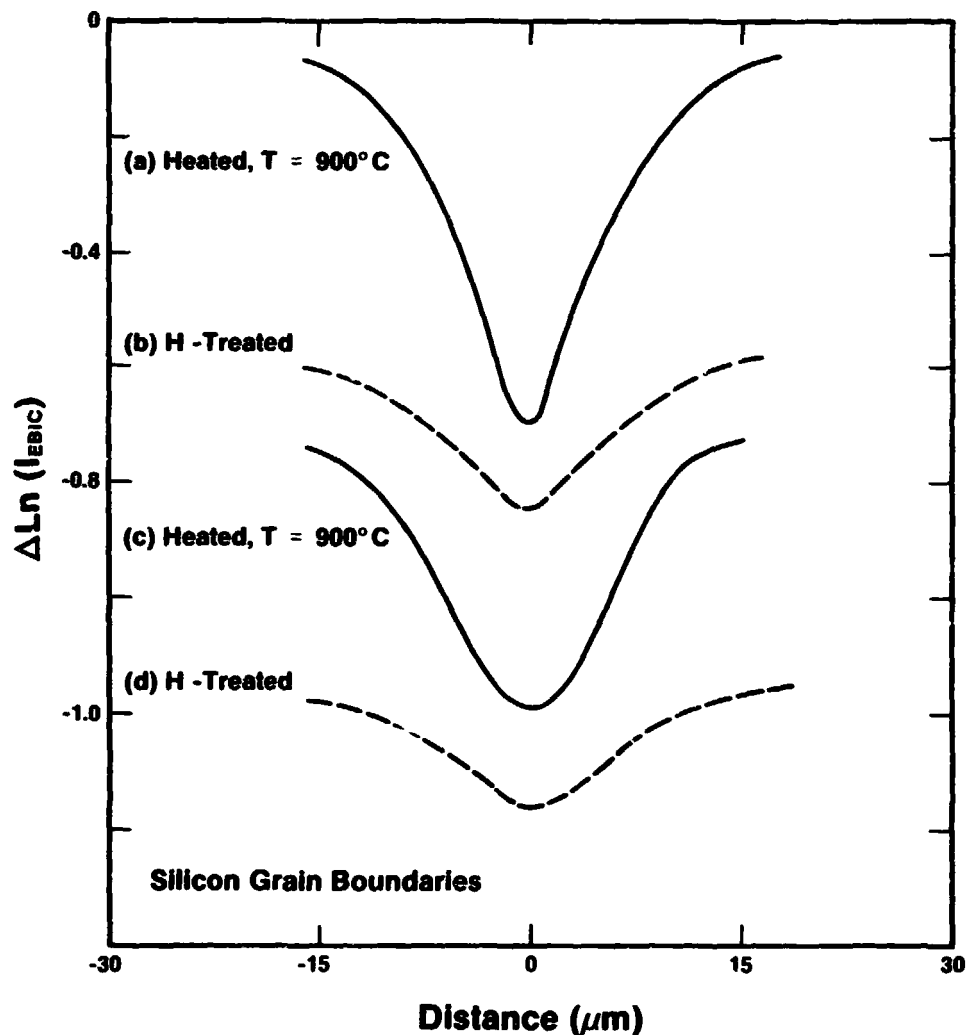


Fig. 9. EBIC linescans for Si grain boundary: (a) annealed at 900°C, for 30 min. in Ar; (b) H<sub>2</sub>-passivated, 4 min. 275°C; (c) reheated, T = 900°C, 30 min. in Ar; and, (d) H<sub>2</sub>-passivated again.

This interaction is illustrated in the SIMS area maps of Figs. (13-15). A computer-processed SIMS map sequence of the intersection of the grain boundary with the wafer surface is presented in Fig. 13. The sample was initially annealed to 900°C, and the boundary contains a high oxygen content. Hydrogen decoration of the region is noted after 1 min of the passivation processing. Figure 13c shows almost complete hydrogen decoration after 2 min of processing. Using the technique to examine the grain boundary composition within plane described earlier in this paper, the penetration of the hydrogen down the boundary plane as a function of processing time is evidenced in Fig. 14 for passivation treatments of 0.5, 1, 3, 4 and 6 minutes. The grain boundary was annealed initially to 900°C. The relatively high initial heat treatment pro-

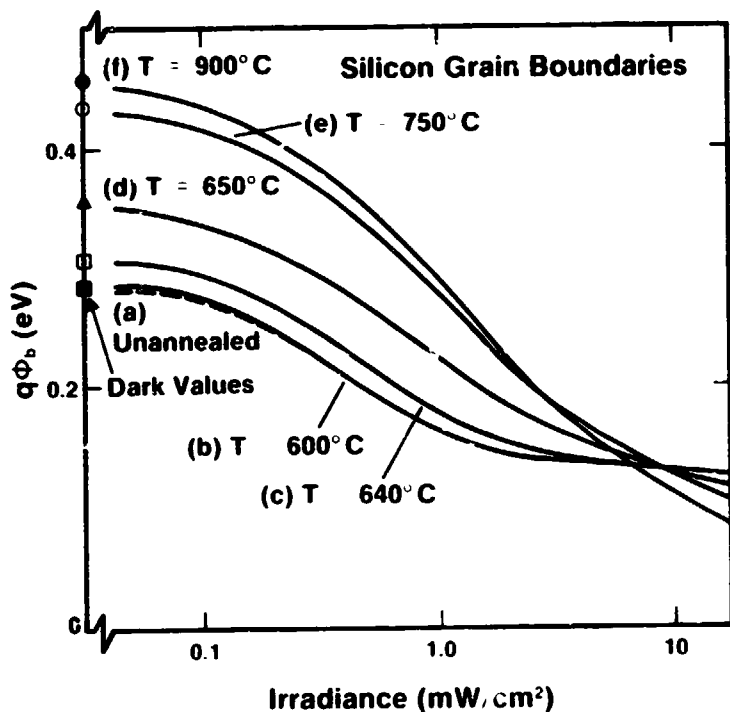


Fig. 10. Dependence of grain boundary barrier potential on light irradiation level for unannealed grain boundary in sequence of alternate treatments similar to Fig. 9.

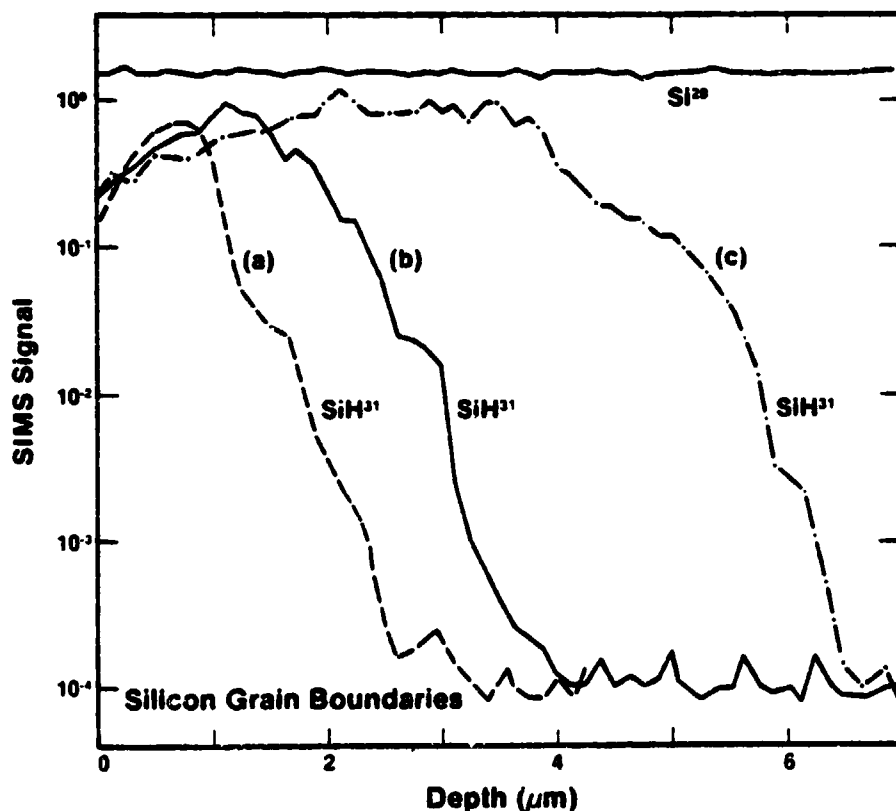


Fig. 11. SIMS depth compositional profile down grain boundary for: (a) 1 min; (b) 2 min.; and (c) 4 min.  $\text{H}_2$ -passivation processed Si.

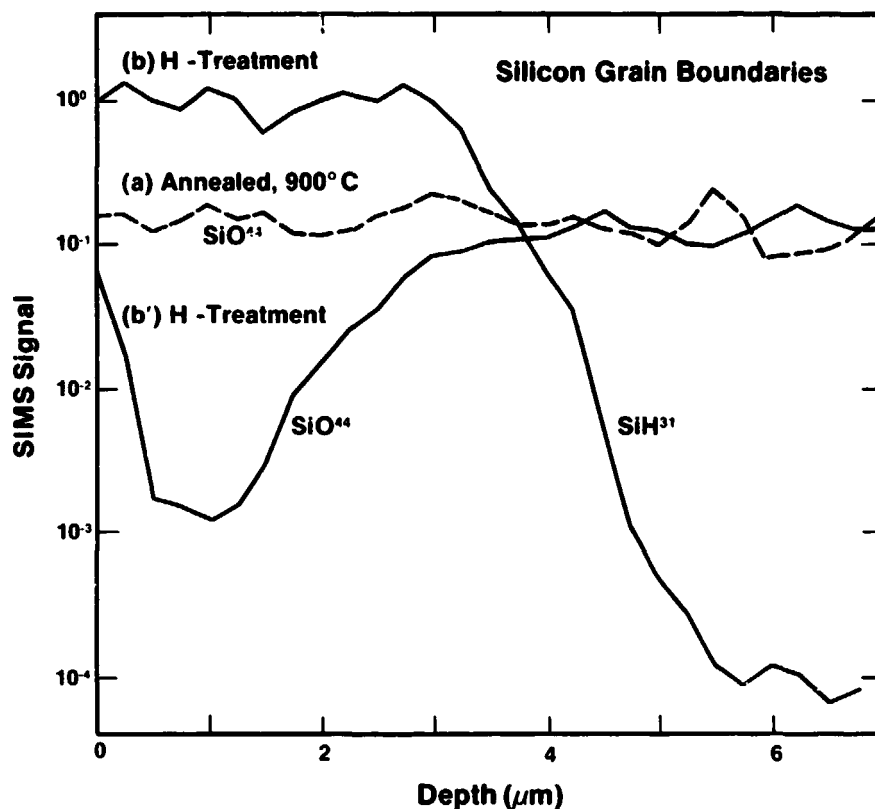


Fig. 12. SIMS depth compositional profile data for: (a) annealed, 900°C, 30 min. in Ar; and, (b)  $\text{H}_2$ -passivated processed Si grain boundary. (b') shows oxide level as function of depth after  $\text{H}_2$ -treatment.

vides for a high oxygen content of the boundary. The interaction of the hydrogen with the oxygen present at the boundary is better illustrated in the grain boundary of Fig. 15. This sample had been annealed to 750°C before the passivation process, and the oxygen at the boundary is somewhat less than the previous case. The hydrogen incorporation is observed to be enhanced in those regions that initially are oxidized. The exact chemistry of this process is not known. Methods similar to the specialized SIMS technique are currently being developed (e.g., digitally-resolved EELS) in order to investigate the chemical interaction of the species in-situ, during the treatments.



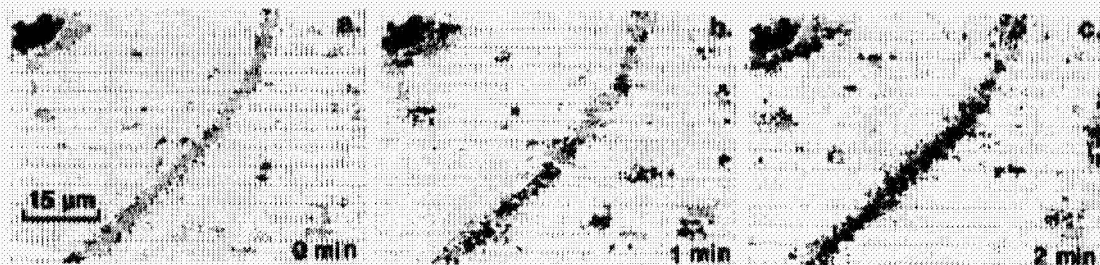


Fig. 13. SIMS mapping sequence of grain boundary intersection with wafer surface as function of passivation time showing decoration of boundary with hydrogen.

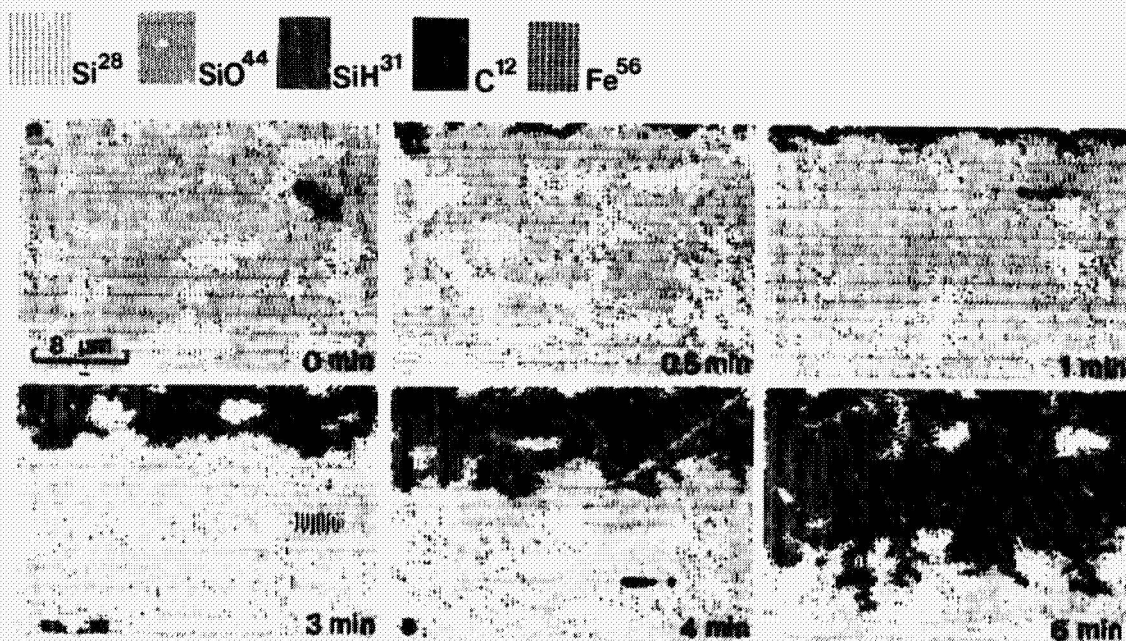
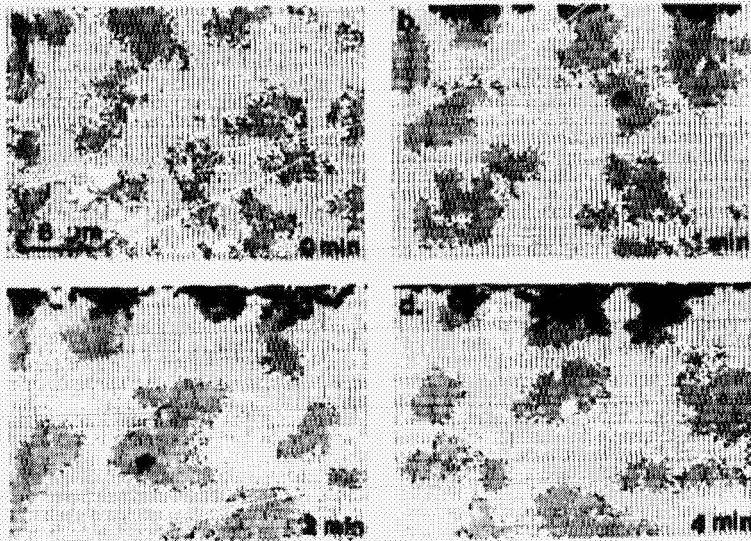


Fig. 14. SIMS mapping sequence showing hydrogen penetration of grain boundary plane as a function of passivation processing time. Grain boundary heated to 900°C before passivation.



ORIGINAL PAGE IS  
OF POOR QUALITY

*Fig. 15. SIMS mapping sequence showing hydrogen - oxygen interaction at grain boundary heated to 750°C before passivation.*

## V. SUMMARY

The detection of impurities in silicon using AES and SIMS has been demonstrated, and the correlation of impurities with microelectrical characteristics has been exemplified. The interrelationships among grain boundary impurity species, grain boundary electrical properties and solar cell performance in polycrystalline Si have been demonstrated. Specifically, two impurity mechanisms have been evaluated: (i) the segregation of oxygen to the intergrain regions during heat treatments; and, (ii) the incorporation of hydrogen in these regions during the passivation process. Finally, a specially-developed SIMS impurity mapping technique has been introduced which, for the first time, allows the investigation of the composition of a grain boundary surface utilizing volume indexing during the SIMS profiling.

## Acknowledgement

The author gratefully acknowledges the inputs, assistance and work of J.R. Dick, R.J. Matson, T.P. Massopust, P.J. Ireland and A. Swartzlander of SERI, all of whom contributed greatly to the work of this paper. The author is also grateful to D.W. Ritchie of SERI for his encouragement of this work. This work was supported by the U.S. Department of Energy under Contract Number EG-77-C-01-4042.

## REFERENCES

1. See, for example, A.W. Czanderna, et al., Methods of Surface Analysis (Elsevier Scientific, New York; 1975).
2. L.L. Kazmerski, Proc. 17th IEEE Photovoltaic Spec. Conf., Orlando (IEEE, New York; 1984) (in-press).
3. D. Redfield, Appl. Phys. Lett. 38, 174 (1981).
4. L.L. Kazmerski and J.R. Dick, J. Vac. Sci. Technol. A2, 1120 (1984).
5. L.L. Kazmerski, Proc. 5th EC Solar Photovoltaic Conf. (Reidel, 1984) (in-press).
6. J.I. Hanoka, C.H. Seager, D.J. Sharp and J.K.G. Panitz, J. Appl. Phys. 42, 618 (1983).
7. C. Dube, J.I. Hanoka and D.B. Sandstrom, Appl. Phys. Lett. 44, 425 (1983).

## DISCUSSION

LOFERSKI: Toward the surface part of the Green cell, it's certainly a little bit astonishing, isn't it, that the phosphorus concentration is decreasing as you go toward the surface? Is that what you really meant or did you say it backwards?

KAZMERSKI: I think that in most SIMS data you will see a slight decrease in the signal right toward the surface. The whole thickness of the phosphorus region we showed there is only about 2000 Å.

LOFERSKI: And how about the thickness of the oxide region? What did you say it was, greater than 20 Å?

KAZMERSKI: Well it should be about 20 Å but if you look there, it looks like the data is spread out and it looks more like 50 or 60 Å.

LOFERSKI: So it is 50 or 60 Å, is what you would estimate?

KAZMERSKI: Yes, I am sure it is about 50 or 60 Å.

LOFERSKI: But you are saying that as you go toward the surface, even in an ordinary cell, if you did it with this volume indexing, you would find a decrease in the phosphorus concentration?

KAZMERSKI: Yes. I think so. You are seeing about 500 Å, that region that it decreases from  $20^{20}$  down to  $10^{18}$   $\text{cm}^{-3}$ .

LOFERSKI: Yesterday Larry Olsen was showing some comparisons of a spreading resistance measurement profile and a SIMS profile, and there is a significant difference in the way they look. You mentioned being careful about using SIMS profiling because of the damage it does. If you compare a spreading resistance with a SIMS profile, which you would recommend as the more likely one to be correct?

KAZMERSKI: It depends on what you are looking for. Certainly one wouldn't want to measure resistance using SIMS, but for a pure representation of the profile, if the SIMS is done correctly, I'd would go with the SIMS.

LOFERSKI: I guess that actually his profile did show a drop-off at the surface too, as I recall.

MILSTEIN: The RCA SIMS profile showed it going up all the way to the surface.

To change the subject on you, you mentioned in terms of your SIMS resolution that you could resolve mass peaks for different species which had the same mass-to-charge ratio, for example, 31, phosphorus, and three silicon species, and quite frankly I am quite curious as to how that is done and whether you care to comment on it.

KAZMERSKI: You mean how to resolve it?



**MILSTEIN:** Well, if you had the same charge-to-mass ratio, and going through something like a quadripole mass analyzer.

**KAZMERSKI:** It's not a quadripole. This is a magnetic sector. You would never be able to do it in a quadripole. You just have the mass separation. It is done with a magnetic sector and this is all done on the Camaca system. So you have your mass resolution as something like 50,000. It is not a quadripole. You would never be able to get that mass resolution with a quadripole. On a quadripole it would look just like one peak. In fact, on some quadripoles that we have seen, the mass resolution even drops off as a function of the time to mass, and sometimes you get an overlapping of two masses.

**CAMPBELL:** Have you looked at the hydrogen distribution as a function of depth in any single-crystal silicon?

**KAZMERSKI:** We looked at -- not really in single-crystal -- we looked at the grain regions in the silicon material here too, you know in the adjacent grain, and did not see any penetration. As a matter of fact, what we saw was some interaction with the oxide that might have been present right on the surface, but not a penetration into the grains.

**CAMPBELL:** There was some indication at the last PVSC that there was a bulk effect with hydrogen passivation.

**KAZMERSKI:** Yes. I heard that too, and we talked to the people and I think the penetration on the grains was not significant.

**KEAVNEY:** I wanted to ask about the low-temperature-annealed samples that have unactivated grain boundaries. What was their thermal history before they were annealed?

**KAZMERSKI:** I should go back. What we are doing is looking at one grain boundary of an unannealed sample. It doesn't mean that there weren't active grain boundaries also in that sample. We selected one that was not active to begin with. Its thermal history was that this was a directionally solidified sample with a grain size of about one-half to three-quarters of a centimeter that had not seen any processing beforehand, forming the junction for EBIC was done by a low-temperature oxidation at about 100°C. So that is the highest temperature the device had seen before any electrical measurements were taken.

**KEAVNEY:** Do you know how quickly it was cooled from the melt?

**KAZMERSKI:** No.

**KEAVNEY:** How quickly was the temperature cooled from the samples that were annealed at 900°C?

**KAZMERSKI:** The annealing procedure was to remove them from the annealing furnace and they were probably cooled over one-half hour or so.

**RAI-CHOUDHURY:** You mentioned hydrogen passivating defects; apparently oxygen

is active in it. I have two questions: Did you look at this defect by DLTS as to what kind of defect level it is? The other question is: Do you feel that oxygen was present in a precipitated form, rather than a single point defect, for it to be activated or deactivated? Can you make any comments on those?

**KAZMERSKI:** The first one: We did not do any DLTS on those things so I have no idea. I think that the people at SERI who had been doing DLTS on this polycrystalline material -- it is not a very satisfying measurement. You really have to spend a lot of time, so when the people attempted to do some DLTS, it looked like it was very difficult to identify any levels. I am sorry, I missed your second question.

**RAI-CHOUDHURY:** I have a lot of concern about oxygen, what it is doing to silicon, Czochralski silicon, and so forth. Does the oxygen, for it to be passivated by hydrogen -- it seemed like it should be present as it precipitated -- or can it react with hydrogen if it is present in the point defect without a cluster, without a precipitation?

**KAZMERSKI:** I really can't answer that, but I see no reason why not, if you look at the hydrogen and see there are also some point defects and other defects in there which are decorated by oxygen. The hydrogen seems to passivate those too, so I guess that would be true.

By the way, something in here, even though we see the hydrogen going down the grain boundary, there is still oxygen in the background. It is not like the oxygen is coming off, when the hydrogen goes the oxygen is leaving. There still is oxygen present.

**TAN:** If I may make a comment. Normally oxygen in silicon is not electrically active. Very difficult to pick up any level by the DLTS. So I believe, really, that we simply don't know what we are passivating. Where is this hydrogen? And the final thing is to say some form of dangling bond -- whether they are related to oxygen or not -- I don't think that question can be settled at this moment.

**KAZMERSKI:** I think that all we can do is say, there is the existence of oxygen and hydrogen, and there is some interaction between the two species.

**WOLF:** You answered only one part of my question, namely, the oxygen is still there until the hydrogen comes, but as you showed, as you increase the annealing temperature, more and more oxygen appears. Now where does it come from? Is it just activated so it becomes visible, or does it diffuse there from the outside, from the atmosphere, like the hydrogen comes in from the outside, or does it come out of the crystal?

**KAZMERSKI:** Well, presumably, it comes from the crystal. The annealing has been done in vacuum and it has been done in argon, it has been done in nitrogen, in a controlled atmosphere, so it is doubtful that it is coming from outside, and we presume that it is coming from the inside. Once again, the level here is about  $10^{17} \text{ cm}^{-3}$  of oxygen.

WOLF: Which is probably an order of magnitude less than what you would expect to be present in Czochralski, if it is a Cz type crystal.

KAZMERSKI: Or an order of magnitude more.

WOLF: You expect around  $10^{18} \text{ cm}^{-3}$  usually, don't you?

KAZMERSKI: I guess, at least in these data, the bulk data shows about  $10^{16} \text{ cm}^{-3}$ .

WOLF: Another comment I want to make is with respect to the Green cell. It seems your cross section was done not under the metal contact, but in between the contacts, and there should be about 100 to 200 Å of oxide, not 20 Å. There is a thicker oxide between the contacts normally. The 20 Å are only under the contacts.

KAZMERSKI: These data might be correct but the surface was thicker than 20 Å. I said more like 60 Å.

WOLF: Yes. That is what you said.

OLSEN: I think it is between 50 and 100 Å, is where he is using now. Between the contacts. That is what I was going to say.

KAZMERSKI: Well, then the data might be OK.

OLSEN: I have another question. Was that a zinc sulfide and magnesium fluoride? Is that the correct order? Is zinc sulfide on top? It is usually the other way around.

HANOKA: What is your sensitivity for oxygen? Isn't it around the low  $10^{17} \text{ cm}^{-3}$ ? At least that is what I hear from Evans who does SIMS, out on the West Coast.

KAZMERSKI: It is  $10^{16} \text{ cm}^{-3}$ .

HANOKA: So yours is better than that, then. Second question: When you do this volume imaging, you showed a picture of your sputtering, basically a perfect parallel pipe, and in fact when you sputter your volume isn't it a thing where your sides slope? And isn't that sputter in that shape also a function of material when you are sputtering?

KAZMERSKI: What I am doing is only collecting the data from that rectangle. The sputtering may be more than that but the data are only being recorded from that rectangle.

HANOKA: So you are picking your rectangle within the sputter volume.

KAZMERSKI: That is correct.

QUESTION: I wanted to go back to Joe Loferski's question on the profile. You indicated that the concentration of the phosphorus fell off near the surface, but I didn't understand whether that was an artifact of the



measurement or whether you think that that is, in fact, what is happening to the profile.

KAZMERSKI: I think that is what is happening to the profile. Right near, within 500 Å of the surface, it drops off a little and then comes up and then goes down.

RAO: It seems to me that when the hydrogen passivates, not all grain boundaries are passivated equally. Now, do you have a characterization of these grain boundaries? Which kind of grain boundaries get deactivated with the hydrogen and which don't?

KAZMERSKI: We have seen that same thing. The only data I have showed you here is to be able to represent the volume indexing and attrition, but I think that is true that the grain boundaries are being affected differently. In fact, the only grain boundaries we are working with here are medium-angle grain boundaries, and I should point that out too. There is about a 28 or 30 degree mismatch between the  $\langle 111 \rangle$  angles and the two grains. So that it could very well be that the structure of those grain boundaries is different, if you go to low-angle grain boundaries or even to higher-angle grain boundaries which will have different electrical properties.

RAO: Another question, which has to do with Martin Wolf's question. As you go away from the grain boundary do you find a concentration gradient of the oxygen, can we see it?

KAZMERSKI: Yes. You can do the same sort of thing. As you go away from the boundary itself you can see the decrease in oxygen concentration.

RAO: So can you calculate the diffusion coefficient and see if it matches up with the bulk diffusion coefficient of oxygen in silicon?

KAZMERSKI: You could do that. I never thought of that but you could do that.

GRUNTHANER: When I have looked at silicon oxide structures that have seen ion beams, whether those ion beams be argon systems or they be cesium systems, there is substantial generation of intermediate oxidation states from silicon sputtering mixing. Now, in the data you are showing here, in these grain boundaries in the oxygen and hydrogen passivation, they are quite clearly being taken on the same sample in the same general area where you are then exposing the system subsequently to the hydrogen. Now my question is, to what extent do you expect there is a degree of activation of the ion beam interactions with the oxygen going on to the subsequent decoration that you are seeing with the hydrogen, since presumably you are doing this in a static mode?

KAZMERSKI: First of all, each one of those hydrogen cases is for a separate sample of a grain boundary that has been cut and divided so the hydrogen passivation was done separately on each one. So it is not the same grain boundary in that case. You can see if you look at it that there are different structures. As a matter of fact, when the carbon that is present at some of the regions are not the same grain boundary itself, it is a

sequence of six grain boundaries that are cut in sequence going across. They are in the same grain boundary length but the grain boundary is cut into six adjacent pieces. It is not the same region each time. So it is not passivated. And then measure, because as soon as you measure it you are done with that sample.